








Evolution of Ycf54-independent chlorophyll biosynthesis in cyanobacteria

Guangyu E. Chen^a , Andrew Hitchcock^a , Jan Mareš^{b,c,d} , Yanhai Gong^e , Martin Tichý^{b,d}, Jan Pilný^b, Lucie Kovářová^b, Barbora Zdvihalová^b, Jian Xu^e , C. Neil Hunter^a , and Roman Sobotka^{b,d,1} 

^aDepartment of Molecular Biology and Biotechnology, University of Sheffield, Sheffield S10 2TN, United Kingdom; ^bInstitute of Microbiology, Czech Academy of Sciences, 37901 Třeboň, Czech Republic; ^cInstitute of Hydrobiology, Biology Centre of the Czech Academy of Sciences, 37005 České Budějovice, 4.75570.0894T

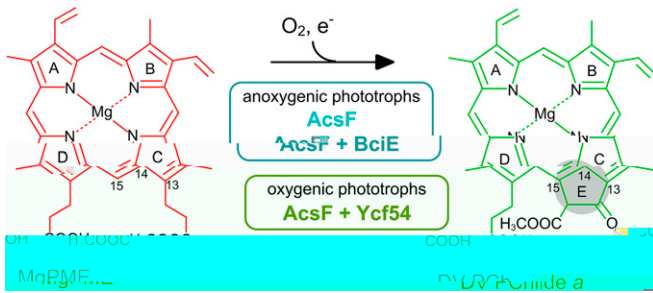


Fig. 1. The O_2 -dependent MgPME cyclase reaction. In most anoxygenic phototrophs, AcsF is the only subunit required for formation of the isocyclic E ring (highlighted). Alphaproteobacterial AcsF requires an auxiliary subunit (BciE) for activity, and another auxiliary subunit (Ycf54) is required for cyclase activity in oxygenic phototrophs. e^- represents the electron donor to the diiron center of AcsF. The relevant macrocycle carbons are numbered according to the International Union of Pure and Applied Chemistry.

Synechocystis Ycf54 copurifies with both CycI and CycII (9) and the single AcsF homolog in higher plants also interacts with Ycf54 (10, 11). Inactivation of the *ycf54* gene strongly impairs cyclase activity (12) and Ycf54-less mutants exhibit severe phenotypes, including lower levels of the AcsF subunit, a buildup of the cyclase substrate MgPME, and lower synthesis of DV PChlide *a* and Chls (9–11, 13). The strict requirement of Ycf54 for the cyclase activity *in vivo* has also been demonstrated by heterologous coexpression of *Synechocystis*, algal, and plant CycI/AcsF enzymes with their cognate Ycf54 in *E. coli* and in *Rvi. gelatinosus* (14). However, the exact role of Ycf54 remains enigmatic, and a possible catalytic function has not been tested due to the absence of an *in vitro* cyclase assay. It is noteworthy that, in contrast to all other cyanobacteria, low-light (LL) ecotypes of *Prochlorococcus* do not contain Ycf54 (15); thus, a Ycf54-independent cyclase evolved naturally in these abundant marine microorganisms.

In the present study, we used adaptive laboratory evolution to generate a Ycf54-independent cyclase in the model cyanobacterium *Synechocystis*. By placing a *Synechocystis* $\Delta ycf54$ mutant under selective pressure, we isolated two strains where cyclase activity and Chl biosynthesis were restored. Genome sequencing revealed the changes necessary to compensate for the lack of Ycf54 in these suppressor mutants were a D219G substitution in CycI and inactivation of a putative esterase, Slr1916. We present evidence that Ycf54 is required for both normal accumulation of

CycI and full cyclase activity. The Slr1916 protein also affects the CycI level and activity, but the mechanism seems to be indirect through up-regulation of the whole Chl biosynthetic pathway. *Synechocystis* was also used as a host to test the activity of cyclase enzymes from the marine picocyanobacterium *Prochlorococcus* in the presence and absence of Ycf54. The role of Ycf54 and the evolution of the O_2 -dependent cyclase reaction are discussed.

Results

Identification of Mutations Suppressing the Deletion of the *ycf54* Gene. The $\Delta ycf54$ mutant of *Synechocystis* has severely impaired Chl biosynthesis (~13% of wild-type [WT] Chl levels) and is incapable of photoautotrophic growth (12). We reported previously that the purple bacterial cyclase gene from *Rvi. gelatinosus*, *acsF^{Rg}*, complemented the loss of *cycI* in *Synechocystis*, irrespective of the presence of Ycf54 (6). The photoautotrophic growth rate of complemented strains was comparable with the WT under 30 $\mu\text{mol photons}\cdot\text{m}^{-2}\cdot\text{s}^{-1}$ (Fig. 2A) (see *SI Appendix, Table S1* for list of strains and plasmids described in this study). The presence of the foreign *acsF^{Rg}* does not affect the distribution of Ycf54 between membrane and soluble fractions, nor is the level of *acsF^{Rg}* protein or its association with membranes affected by the absence of Ycf54 (Fig. 2B). However, complemented strains did suffer from growth retardation when the light intensity increased to 400 $\mu\text{mol photons}\cdot\text{m}^{-2}\cdot\text{s}^{-1}$ (hereafter referred to as HL for high light) (Fig. 2A), indicating the advantage of the native CycI-Ycf54 couple under less favorable growth conditions.

Such observations led us to explore whether photoautotrophy could be restored to the $\Delta ycf54$ mutant through adaptive evolution. We incubated the mutant on BG11 agar without glucose under 15 $\mu\text{mol photons}\cdot\text{m}^{-2}\cdot\text{s}^{-1}$; after 3 wk, a few tiny colonies arose and were restreaked onto a new plate and incubated under 30 $\mu\text{mol photons}\cdot\text{m}^{-2}\cdot\text{s}^{-1}$. The restreak procedure was repeated every fortnight, and after 12 wk two photoautotrophic strains were isolated with Chl levels (monitored at ~680 nm) similar to the WT (see *SI Appendix, Fig. S1* for whole-cell spectra), designated suppressor mutant 1 (SM1) and SM2.

Next-generation sequencing was used to analyze the genomes of SM1 and SM2, together with the “parent” $\Delta ycf54$ mutant and the isogenic WT strain (GT-W) (16). Variants were identified by mapping the obtained sequences to a reference strain GT-S (17). Those found in SM1 or SM2 but not in the $\Delta ycf54$ strain were identified as putative suppressor mutations and are listed in *SI Appendix, Table S2*. Intriguingly, both SM1 and SM2 contain mutations in the *cycI* gene and in an open reading frame, *slr1916*.

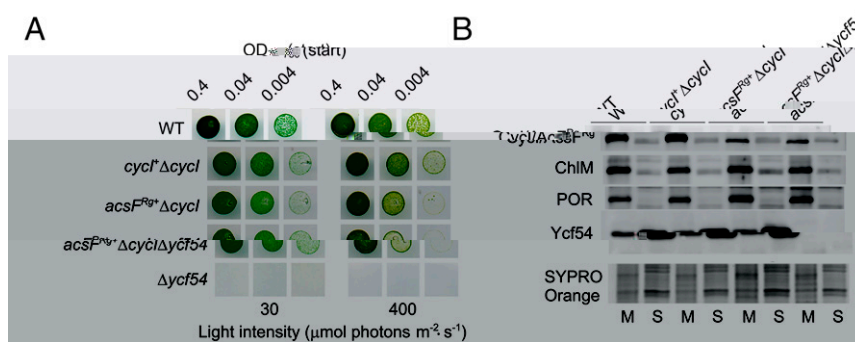


Fig. 2. Analysis of *Synechocystis* mutants complemented with the *Rvi. gelatinosus* cyclase gene (*acsF^{Rg}*). (A) Drop growth assays of the described strains grown on BG11 agar under the indicated light intensity. The *cycI⁺ ΔcycI* strain, which expresses the native *cycI* gene under the control of the *psbAII* promoter, is shown as a control for the expression method. Photographs were taken after incubation for 6 d. (B) Immunodetection of selected Chl biosynthetic enzymes in the indicated strains. Membrane (M) and soluble (S) protein fractions were isolated from an equal number of cells from each strain grown under 30 $\mu\text{mol photons}\cdot\text{m}^{-2}\cdot\text{s}^{-1}$. CycI and *acsF^{Rg}* were detected by an antibody raised against the Arabidopsis AcsF homolog, which cross-reacts significantly less strongly with *acsF^{Rg}* than with CycI (*SI Appendix, Fig. S11*). Part of the SDS-PAGE gel was stained with SYPRO Orange as a loading control.

A D219G substitution in *CycI* is shared by SM1 and SM2, while *slr1916*, provisionally annotated to encode a 283-aa esterase, is truncated due to frameshifts that leave 129 and 104 aa intact in SM1 and SM2, respectively.

D219G Substitution in *cycI* or Inactivation of *slr1916* Individually Restore Photoautotrophy to the $\Delta ycf54$ Mutant. To determine the contribution made by the D219G substituted *CycI* (hereafter *CycI*SM) to the observed suppressor effects, we constructed a $\Delta ycf54$ *cycI*^{SM+} strain in which the redundant *psbAII* gene was replaced with the *cycI*SM mutant gene (see *SI Appendix, Fig. S2* for colony PCR screening of *Synechocystis* strains). A strain expressing *cycI*SM in the WT background and another strain, $\Delta ycf54$ *cycI*⁺ expressing an extra copy of the native *cycI* gene, served as controls. Remarkably, the $\Delta ycf54$ mutant complemented with the *cycI*SM gene was able to grow photoautotrophically even under HL (Fig. 3A), and its Chl level, although still not matching the WT level, increased dramatically when compared with $\Delta ycf54$ (Fig. 3B). Complementation of the *ycf54* mutant phenotypes was not due to increased dosage as the

control $\Delta ycf54$ *cycI*⁺ strain still has very low levels of Chl and was unable to grow in the absence of glucose (*SI Appendix, Fig. S3A*). The growth of $\Delta ycf54$ *cycI*^{SM+} was close to the WT under 100 $\mu\text{mol photons}\cdot\text{m}^{-2}\cdot\text{s}^{-1}$ (Fig. 3A), and this was used as standard light (SL) intensity for the remainder of the study.

We also constructed $\Delta ycf54$ *slr1916*SM and $\Delta ycf54$ Δ *slr1916* strains in which *slr1916* was either truncated, resembling the SM1 mutation, or deleted, respectively. The two strains appeared identical, with Chl contents (*SI Appendix, Fig. S3B*) notably higher than the $\Delta ycf54$ strain but lower than the $\Delta ycf54$ *cycI*^{SM+} strain (Fig. 3B). The improvement achieved by inactivation of *slr1916* was thus less prominent than with the *cycI*SM mutation and the $\Delta ycf54$ *slr1916*SM strain grew more slowly under SL and HL than the $\Delta ycf54$ *cycI*^{SM+} strain.

In an attempt to reproduce the phenotypes of the suppressor mutants, we combined the two suppressor mutations to make a $\Delta ycf54$ *cycI*^{SM+} *slr1916*SM strain. These mutant cells grew better than the $\Delta ycf54$ *cycI*^{SM+} strain under 30 $\mu\text{mol photons}\cdot\text{m}^{-2}\cdot\text{s}^{-1}$, the light intensity used for generating the suppressor mutants, but less well under SL and HL (Fig. 3A). Whole-cell absorption

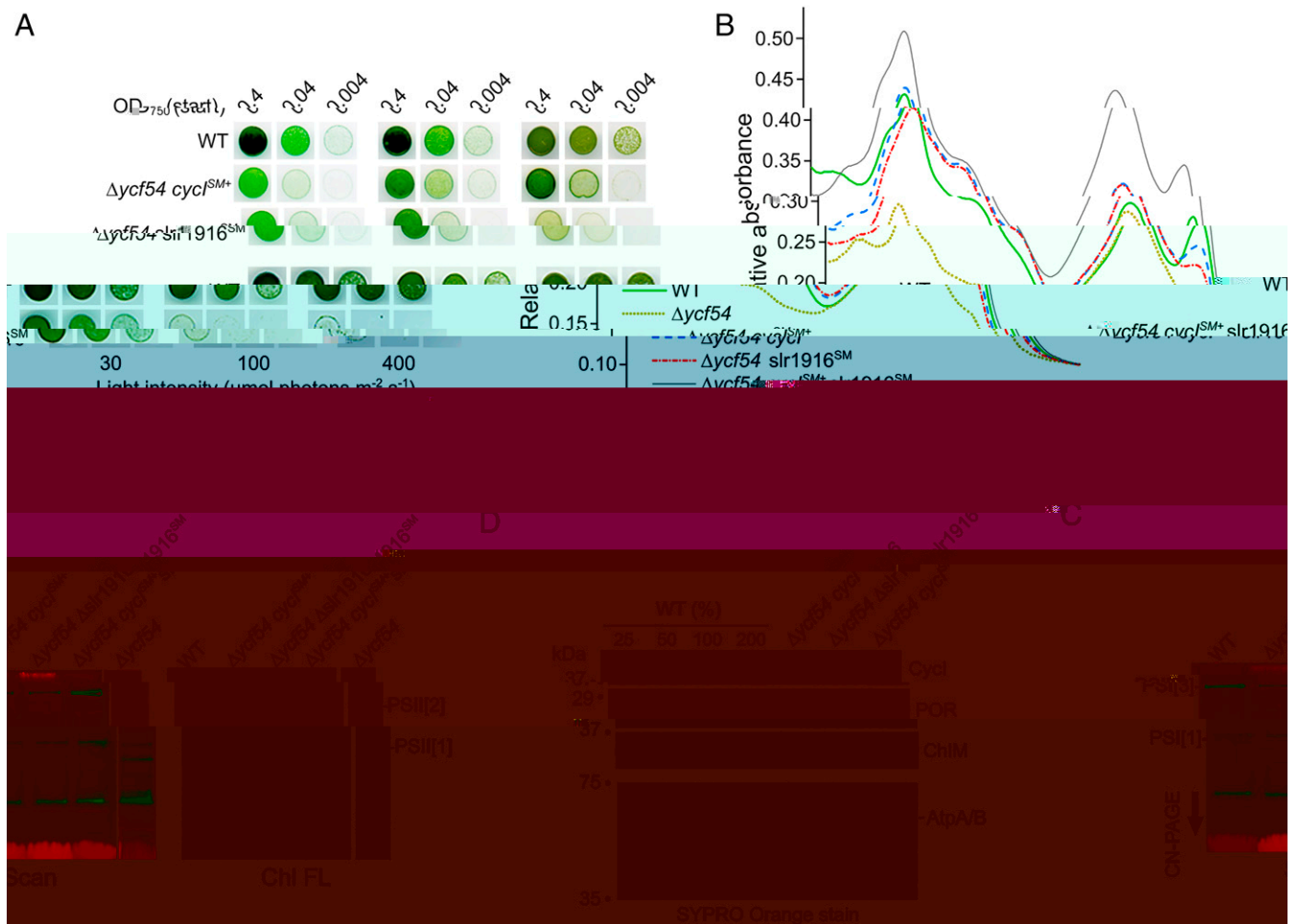


Fig. 3. Analysis of the *Synechocystis* $\Delta ycf54$ mutant complemented with single and double suppressor mutations. (A) Drop growth assays of the described strains grown on BG11 agar under different light intensities. Photographs were taken after incubation for 6 d. (B) Whole-cell absorption spectra of the described strains grown autotrophically under SL, except the $\Delta ycf54$ strain, which was grown mixotrophically under LL. (C) CN-PAGE separation of membrane proteins isolated from the described strains. The growth conditions were as described in B. The loading corresponds to the same number of cells from each strain, except the $\Delta ycf54$ strain, for which four times the number of cells were loaded to detect traces of PSII in this strain. Pigmented complexes were detected by their color (Scan) and Chl fluorescence with excitation by blue light (Chl FL). PSI[1] and PSI[3] indicate monomeric and trimeric PSI, respectively; PSII[1] and PSII[2] indicate monomeric and dimeric PSII, respectively. See *SI Appendix, Fig. S4* for the second-dimension separation of selected CN-gel strips by SDS-PAGE. (D) Immunodetection of selected Chl biosynthetic enzymes in the indicated strains. Membrane fractions were isolated and analyzed by SDS-PAGE with loading on an equal cell number basis, followed by immunodetection. The WT sample was also loaded at 25%, 50%, and 200% levels for ease of comparison. Part of the SDS-PAGE gel was stained with SYPRO Orange as a loading control.

spectra show that the truncation of *slr1916* in the $\Delta ycf54$ *cycI*^{SM+} strain further increased accumulation of Chl, as well as that of phycobilisomes, to a level significantly higher than in the WT (Fig. 3B). Despite the presence of other putative suppressor mutations in SM1 and SM2 (see *SI Appendix, Table S2* for list of identified suppressor mutations), these data suggest that the combination of the D219G substitution in *cycI* and the truncation of *slr1916* principally account for the suppressor effects observed in SM1 and SM2.

Accumulation of Chl-binding proteins in the strains described above was analyzed by clear-native polyacrylamide gel electrophoresis (CN-PAGE). Visibly green bands and detection of Chl fluorescence showed that both photosystem I (PSI) and photosystem II (PSII) levels were partially restored in the $\Delta ycf54$ *cycI*^{SM+} and $\Delta ycf54$ $\Delta slr1916$ strains (Fig. 3C). In the $\Delta ycf54$ *cycI*^{SM+} *slr1916*SM strain, the PSII level was similar to WT and there was a noticeably higher level of PSI (Fig. 3C), which was further supported by two-dimensional CN/SDS-PAGE analysis of membrane complexes (*SI Appendix, Fig. S4*). There was no apparent effect of expressing the *cycI*SM gene in the WT background (see *SI Appendix, Fig. S5 A–D* for the comparison between the WT and *cycI*^{SM+} strains).

The accumulation of Chl biosynthetic enzymes is severely hindered in the $\Delta ycf54$ mutant, which contains only ~15% of WT CycI levels and ~50% the level of POR (12). Our immunoblot analysis revealed that expression of the *cycI*SM gene increased the levels of CycI and POR (Fig. 3D). On the other hand, inactivation of *slr1916* only had marginal effects on the CycI level, but resulted in increased accumulation of POR, with the level in the $\Delta ycf54$ $\Delta slr1916$ and $\Delta ycf54$ *cycI*^{SM+} *slr1916*SM strains being several times higher than in the WT (Fig. 3D).

***Synechocystis* CycISM has Cyclase Activity when Heterologously Expressed in *Rvi. gelatinosus*.** We have shown that the *cycI*SM mutation restored the WT level of CycI in the absence of Ycf54 (Fig. 3D), but it is unclear whether the mutated CycISM has the same catalytic activity as the WT enzyme. As an in vitro assay with purified AcsF has not been reported yet, we assayed the heterologous activity of *Synechocystis* cyclase in a *Rvi. gelatinosus* mutant that lacks both the O₂-sensitive and O₂-dependent cyclase enzymes (6). We grew the *Rvi. gelatinosus* strain expressing *cycI*SM together with a control strain expressing the native *Rvi. gelatinosus* *acsF* gene in liquid culture and monitored the content of BChl *a*. In agreement with the previous report (6), the coexpression of *Synechocystis* *cycI* and *ycf54* is strictly required for the synthesis of BChl *a* (Fig. 4). Intriguingly, there was some residual activity of CycISM in *Rvi. gelatinosus* in the absence of Ycf54, allowing the synthesis of ~1% of BChl measured for the CycI–Ycf54 pair, which was boosted to ~50% by the inclusion of Ycf54 (Fig. 4). These results show that CycISM can work as a stand-alone cyclase, but still relies on Ycf54 for optimal activity when heterologously expressed in *Rvi. gelatinosus*.

Ycf54 and Slr1916 Affect the Cyclase Level during Nitrogen Deficiency.

To investigate the role of Ycf54 and the effects of the suppressor mutations, we monitored Chl biosynthesis in the WT and complemented strains grown in a nitrogen-fluctuating regime. Nitrogen deficiency is known to diminish the whole tetrapyrrole pathway, and the metabolic flow can be restored quickly (<2 h) upon nitrogen repletion (18). Such regulation requires tightly synchronized levels/activities of all enzymes involved in tetrapyrrole metabolism and any defect in the accumulation/activity of CycI should be much more pronounced than under conditions with sufficient levels of nutrients.

We found that CycI was unstable in the WT during nitrogen deficiency and decreased to ~25% of the predepletion level after 6-h nitrogen deprivation (Fig. 5A), becoming virtually undetectable after 18 h (Fig. 5B). Conversely, ChlM, POR, and Ycf54

were much more stable during nitrogen depletion (Fig. 5B). CycI was still barely detectable after 2-h nitrogen repletion but was restored to the predepletion level after 6 h (Fig. 5B). A similar pattern was observed in the *cycI*^{SM+} strain, confirming that expression of the *cycI*SM gene from the *psbAIII* promoter in the WT background does not alter the level or regulation of the protein (*SI Appendix, Fig. S5E*). We repeated the same experiments with the $\Delta ycf54$ *cycI*^{SM+} and $\Delta ycf54$ *cycI*^{SM+} *slr1916*SM strains. Remarkably, CycI was still present in the $\Delta ycf54$ *cycI*^{SM+} *slr1916*SM strain even after 18-h nitrogen depletion (Fig. 5B). In addition, both complemented strains exhibited a faster recovery of CycI levels upon nitrogen restoration, with a significant CycI signal detectable after only 2 h (Fig. 5B). These results indicate misregulation of the cellular level of CycI in the absence of Ycf54, and that the mutated CycI is stabilized, particularly in combination with the *slr1916*SM mutation.

We also measured the Chl precursor pool to analyze the overall consequence of disruption of the *ycf54* and *slr1916* genes on Chl biosynthesis. Before nitrogen deprivation, the $\Delta ycf54$ *cycI*^{SM+} strain contained approximately four times the amount of MgPME and only half the amount of DV PChlide *a* as the WT, indicating a deficiency in cyclase activity (Fig. 6). This pigment profile is shared by the $\Delta ycf54$ $\Delta slr1916$ strain but with an even higher MgPME level, ~70 times greater than in the WT (Fig. 6),

except for MV Chlide *a* (Fig. 6), which mostly originates from the dephytylation of Chl in the Chl recycling process (19, 20).

Following nitrogen repletion, the WT gradually built up the precursor pool without anomalous accumulation of intermediates, and predepletion precursor levels were restored within 24 h (Fig. 6). In sharp contrast, MgP and MgPME were rapidly restored in the $\Delta ycf54$ *cycI*^{SM+} strain after only 2-h nitrogen repletion and their levels continued to increase up to 12 h (Fig. 6). The fast recovery of CycI in this strain (Fig. 5B) did not result in an abrupt recovery of DV PChlide *a*, which instead built up more gradually (Fig. 6). It seems that the “regreening” process was stalled at the cyclase step, as further evidenced by the drastic

W-10.f0.70c[-0.0cTc729m7537.1

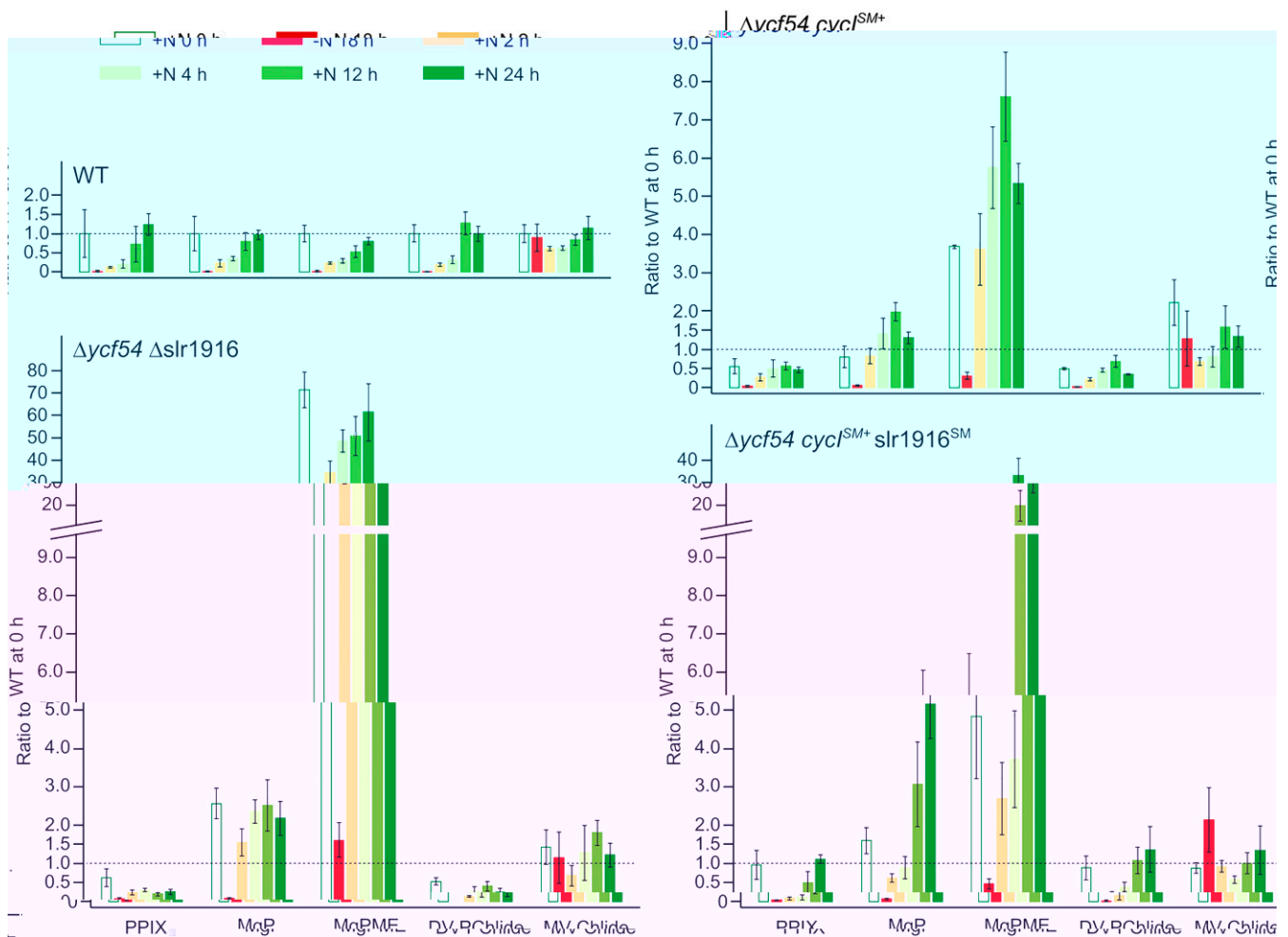


Fig. 6. Analysis of Chl precursors in *Synechocystis* strains recovering from nitrogen depletion. Strains were grown autotrophically under SL and subjected to nitrogen starvation for 18 h, followed by nitrogen repletion by addition of 10 mM NaNO_3 . Pigments were extracted from cells harvested before (+N 0 h) and after (–N 18 h) nitrogen starvation, and after 2, 4, 12, and 24 h of nitrogen repletion. Pigments were analyzed by HPLC to allow detection of protoporphyrin IX (PPIX), Mg-PPIX (MgP), MgP monomethyl ester (MgPME), 3,8-divinyl protochlorophyllide a (DV PChlide), and 3-vinyl chlorophyllide a (MV Chlide). The level of precursors is shown as ratio to the WT level before nitrogen starvation, and the error bars indicate the SD from the mean of biological triplicates.

We did a thorough BLAST search against all cyanobacteria with sequenced genomes (1,048 quality-checked genomes available in the Genome Taxonomy Database [GTDB]) (28) and found that all 89 *Prochlorococcus* genome assemblies clustering in the LL-adapted clades lack the *ycf54* gene. LL-adapted *Prochlorococcus* ecotypes also lack a *bchE* ortholog and so appear to rely solely on an O_2 -dependent cyclase for Chl biosynthesis.

To gain more detailed insight into the evolution of AcsF and Ycf54 in *Prochlorococcus* ecotypes, we constructed a phylogenetic tree inferred from AcsF proteins (394 aligned positions), which was compared to a species tree based on concatenated sequences (3,182 aligned positions) of 13 universally conserved proteins (29) (Fig. 9). Representatives of all phototrophic phyla and LL- and HL-adapted *Prochlorococcus* ecotypes were included. All *Prochlorococcus* ecotypes form a monophyletic lineage within the clade of other picocyanobacteria (marine *Synechococcus* and *Cyanobium*) (Fig. 9). The LL-adapted ecotypes are ancestral in the *Prochlorococcus* lineage and form three paraphyletic branches, whereas the HL-adapted ones form a single compact branch (Fig. 9). The HL-adapted ecotypes contain a typical AcsFI, in keeping with other picocyanobacteria. In contrast, the LL-adapted strains possess only an AcsFII that is phylogenetically distant from other AcsFII proteins (Fig. 9) (see

SI Appendix, Fig. S9 for sequence alignments). Most cyanobacteria contain both AcsFI and AcsFII (*SI Appendix, Fig. S10*); however the latter protein is expressed only under microoxic conditions (30). Apart from *Prochlorococcus* species, most marine *Synechococcus* also contain only one AcsFI homolog (*SI Appendix, Fig. S10*).

To test whether the *acsF* gene from *Prochlorococcus* can function in *Synechocystis*, we expressed the genes from a representative LL-adapted strain, *Prochlorococcus marinus* MIT 9313, and a representative HL-adapted strain, *Prochlorococcus marinus* MED4, in the WT background and subsequently attempted to delete the native *cycI*. We were not able to fully segregate the *acsF*⁹³¹³⁺ Δ *cycI* strain, suggesting that AcsF⁹³¹³ cannot functionally replace CycI in *Synechocystis* under our standard laboratory conditions. This result contrasted with the successful complementation of *Synechocystis* Δ *cycI* strain by the *acsF*^{MED4} gene; although the resulting *acsF*^{MED4+} Δ *cycI* strain still contained low levels of Chl (Fig. 10A), it was able to proliferate autotrophically under SL. On the other hand, the Δ *ycf54* *acsF*^{MED4+} strain showed no improvement in Chl content (Fig. 10B) or autotrophic growth, demonstrating the dependence of AcsF^{MED4} on Ycf54.

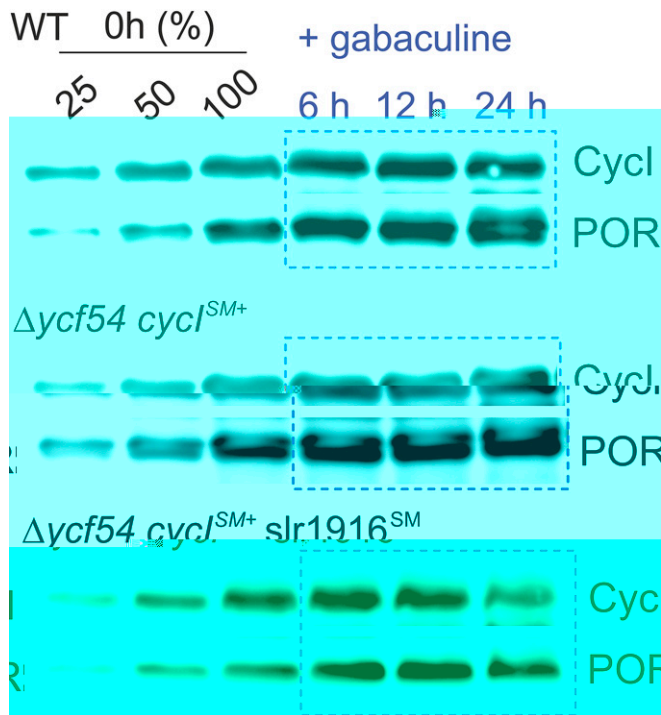


Fig. 7. Immunodetection of Chl biosynthetic enzymes in *Synechocystis* strains before and after treatment with gabaculine. Strains were grown autotrophically under SL. Cells were collected before (0 h) and after 6-, 12-, and 24-h treatment with 5 μM gabaculine. SDS-PAGE analysis and immunodetection were conducted as in Fig. 3D. The 0-h sample was also loaded at 25% and 50% levels for ease of comparison.

The inactivity of AcsF⁹³¹³ in *Synechocystis* is further demonstrated by the phenotype of the $\Delta\text{ycf}54$ *acsF*⁹³¹³⁺ strain, which was unable to grow photoautotrophically and had a Chl level similar to the $\Delta\text{ycf}54$ strain (Fig. 10B). The AcsF⁹³¹³ is, however, of the AcsFII type, and the *Synechocystis* CycII contributes to Chl biosynthesis only under microoxic conditions, likely due to the oxygen-sensitive nature of AcsFII/CycII-type enzymes (7). We therefore tested these strains under low oxygen conditions using a gas mixture containing 2% O₂ and 0.5% CO₂ in N₂ with a light intensity of 30 $\mu\text{mol photons}\cdot\text{m}^{-2}\cdot\text{s}^{-1}$. The $\Delta\text{ycf}54$ *acsF*⁹³¹³⁺ strain exhibited slow autotrophic growth with a doubling time of ~ 95 h, whereas the control $\Delta\text{ycf}54$ *cycII*⁺ strain showed only a negligible increase in turbidity after 5 d. The $\Delta\text{ycf}54$ *acsF*⁹³¹³⁺ strain accumulated significantly more Chl and carotenoids than the $\Delta\text{ycf}54$ *cycII*⁺ strain (Fig. 10C). The observed lack of CycII activity in the $\Delta\text{ycf}54$ *cycII*⁺ strain grown under low oxygen conditions is consistent with the expected dependence of CycII on Ycf54 (9). In summary, our data support a model that the LL-adapted *Prochlorococcus* ecotypes have evolved a distinct Ycf54-independent AcsFII that does not require regulation by Ycf54, a mechanism that is otherwise conserved in cyanobacteria, algae, and plants.

Discussion

In order to investigate the role of Ycf54, we conducted laboratory evolution experiments with the $\Delta\text{ycf}54$ mutant and identified suppressor mutations that restore photoautotrophic growth. Our results clearly demonstrate that a D219G substitution significantly weakens the dependence of CycI on Ycf54 to allow CycI to accumulate without Ycf54, but that Ycf54 is required for optimal cyclase activity. It has been demonstrated that AcsF and Ycf54 form a stable, membrane-bound complex in various model phototrophs (9–11, 31, 32); the docking of Ycf54 onto CycI/CycII

requires a region of positive surface potential on Ycf54 (31). The following enzyme in the pathway, POR, is likely to be a component of the same complex (12, 33), perhaps along with several other Chl biosynthetic enzymes (34); consistently, the absence of Ycf54 in *Synechocystis* destabilizes CycI and POR (9, 12).

Our results support that Ycf54 is required for the stability/accumulation of CycI as well as for optimal cyclase activity in vivo. A recent report shows recombinant barley AcsF does not accumulate in *E. coli* unless coexpressed with Ycf54 (35), indicating a possible role of Ycf54 in the folding and/or maturation of plant AcsF. In addition, *Synechocystis* CycI requires Ycf54 for heterologous cyclase activity in *E. coli* (2) and *Rvi. gelatinosus* (6). On the other hand, Bollivar et al. (36) showed that recombinant Ycf54 stimulates in vitro cyclase activity with barley extracts. A direct role of Ycf54 in the cyclase reaction is further supported by PChlide (Fig. 6) and Chl (Fig. 3B) deficiency in the $\Delta\text{ycf}54$ *cycI*^{SM+} strain, despite restoration of WT-like CycI levels by the D219G substitution (Fig. 3D).

However, why is Ycf54 present in almost all oxygenic phototrophs despite the apparent relative ease for the gene encoding AcsF to mutate to form a Ycf54-independent enzyme? An analogy between the O₂-dependent cyclase and the first committed enzyme in (B)Chl biosynthesis, MgCH, can be drawn here. Although structurally and mechanistically conserved in all phototrophs, MgCH in Chl-producing organisms requires an auxiliary protein, Gun4, which is not found in anoxygenic phototrophs (37, 38), and like the $\Delta\text{ycf}54$ mutant, *Synechocystis* $\Delta\text{gun}4$ mutants have severely lowered levels of Chl (39). Gun4 directly interacts with ChlH, the catalytic subunit of MgCH, and has been shown to control the accumulation of ChlH during the first few hours of recovery from nitrogen depletion (18), enhance enzyme activity in vitro (38, 40, 41), and control the metabolic flux within the tetrapyrrole biosynthesis pathway in cyanobacteria, green algae, and various plant species (37–39, 42, 43).

Given the central importance of Chl for the function of photosynthetic complexes, and the photolability and phototoxicity of its biosynthetic intermediates, multiple layers of regulation are required to adjust production of Chl in response to fluctuating levels of nutrients and light. Apart from MgCH directing PPIX into Chl biosynthesis, the cyclase step is also expected to be tightly regulated. The following enzyme in the pathway, POR, is light activated, and thus its activity is difficult to modulate under fluctuating light. It may therefore be important to control the availability of the POR substrate, i.e., the cyclase product, either by direct intervention in catalysis or controlling the stability of AcsF/CycI. We showed that CycI stability is not impaired by the lack of substrate (Fig. 7), suggesting that the CycI level is controlled by a more sophisticated mechanism that presumably involves Ycf54. Our analysis of the $\Delta\text{ycf}54$ *cycI*^{SM+} strain showed fast recovery of CycI shortly after nitrogen was restored following depletion, which contrasts with the WT-like slower restoration of CycI in the presence of Ycf54 (Fig. 5B and *SI Appendix, Fig. S5E*). We speculate that Ycf54 and Gun4 evolved in cyanobacteria to stabilize and/or regulate the catalytic subunits of Chl biosynthetic enzymes, and later started to modulate the activity of these enzymes providing an additional (strict) measure of control to avoid aberrant accumulation of phototoxic Chl precursors. As photosynthetic bacteria perform anoxygenic photosynthesis and production of BChl is largely controlled by environmental oxygen tension (44), they may not need regulators equivalent to Ycf54 or Gun4.

Intriguingly, unlike other cyanobacteria, the LL-adapted *Prochlorococcus* ecotypes lack the *ycf54* and *acsFI* genes. Given the dependence of CycII on Ycf54 (9) (Fig. 10C and D), we propose that the *acsFI* gene was initially lost in a subpopulation of ancient LL-ecotype *Prochlorococcus*. The loss of *acsFI* can be rationalized, given that the habitat of LL-adapted strains has a low oxygen saturation level as well as low light intensities (45), which

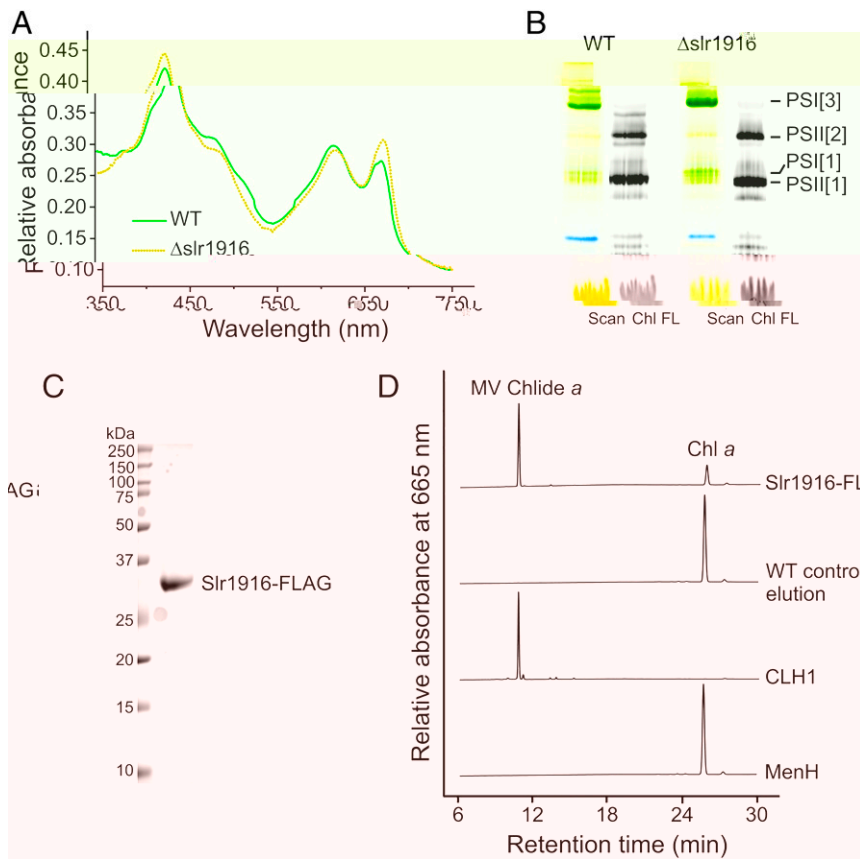


Fig. 8. Analysis of the $\Delta slr1916$ mutant and the Chl dephytylase activity of FLAG-tagged Slr1916 purified from *Synechocystis*. (A) Whole-cell absorption spectra and (B) CN-PAGE separation of membrane proteins isolated from the WT and $\Delta slr1916$ strains grown autotrophically under SL. For CN-PAGE analysis, the loading corresponds to the same number of cells from each strain. Pigmented complexes were detected and annotated as in Fig. 3C. See also [SI Appendix, Fig. S7](#) for the second-dimension separation of CN-gel strips. (C) SDS-PAGE analysis of 15 μ L of purified Slr1916-FLAG from detergent-solubilized *Synechocystis* membranes with protein staining with Coomassie Brilliant Blue staining. (D) HPLC-based in vitro Chl dephytylase assays with Slr1916-FLAG. A positive control using clarified *E. coli* lysate containing Arabidopsis CLH1 ([SI Appendix, Fig. S8B](#)) and negative controls with the FLAG-immunoprecipitation elution from WT *Synechocystis* or purified *E. coli* MenH ([SI Appendix, Fig. S8C](#)) were also performed. Retention times and absorption spectra of peaks were used to identify MV Chlide a and Chl a.

can only support a low rate of oxygen evolution. The remaining AcsFII may then have mutated to become less dependent on Ycf54, allowing a subsequent loss of the *ycf54* gene due to genome streamlining, a well-documented phenomenon in *Prochlorococcus* (46); the likelihood of this mutation event is high, given that we were able to generate a Ycf54-independent mutant of AcsF by laboratory microevolution. The scenario of the HL-adapted ecotypes is completely different as it is unlikely that they could rely on AcsFII for Chl biosynthesis due to the higher levels of oxygen in the upper layers of the oceans. Thus, the HL-adapted ecotypes most likely evolved from a population still possessing *acsFIIycf54* genes by a subsequent loss of *acsFII* (Fig. 9 and [SI Appendix, Fig. S10](#)). Nonetheless, it is notable that, despite extreme genome reduction during the evolution of *Prochlorococcus* species (47), HL ecotypes retain Ycf54. Thus, under high light intensities, the role of Ycf54 appears essential (Fig. 3A).

In contrast to the *cycISM* mutation, inactivation of *slr1916* seems to stimulate the cyclase activity indirectly, rather than by restoring the CycI level (Fig. 3D). After inactivation of the Slr1916 in the $\Delta ycf54$ *cycI^{SM+}* strain, the synthesis of PChlide doubled (Fig. 6) and the cellular Chl level increased significantly (Fig. 3B). However, the resulting strain is more photosensitive (Fig. 3A) and the regulation of the CycI level is disrupted (Fig. 5B). The KEGG database annotates Slr1916 as the MenH enzyme required for phyloquinone biosynthesis, which is supported

by BLAST searches revealing that Slr1916 is the sole homolog of the *E. coli* enzyme in *Synechocystis* (93% coverage, 42% similarity, 29% identity, E value $3e-10$). However, it is worth noting that MenH sequences are highly variable, and only 15 residues were strictly conserved across 47 homologs analyzed by Jiang et al. (48). In plants, mutation of the *menH* locus causes a pale green phenotype due to phyloquinone deficiency, which results in reduced Chl content and stability of PSI (49, 50), and in other *Synechocystis* *men* mutants the absence of phyloquinone results in a lowered level of PSI (51–53). This contrasts with the significantly increased PSI level in $\Delta slr1916$ mutants (54) (Fig. 8B and [SI Appendix, Fig. S7](#)), indicating Slr1916 is not a MenH enzyme. We noticed that Slr1916 contains a GHSLG motif, similar to the PPH motif (GNS[L/I/V]G) identified in plant pheophytinases and Chl dephytylases (25, 26) and the lipase motif (GHSRG) in chlorophyllase (24). Consistently, we found that the purified Slr1916 has Chl dephytylase activity in vitro (Fig. 8D).

We do not expect Slr1916 to be a major Chl dephytylase in *Synechocystis* as during nitrogen starvation the $\Delta ycf54$ *cycI^{SM+}* *slr1916^{SM+}* strain contained high level of MV Chlide a that can only originate from Chl dephytylation (Fig. 6). Screening of an inducible CRISPRi gene repression library in *Synechocystis* identified *slr1916* as one of the few genes that, when down-regulated, leads to significantly increased growth rates in a turbidostat (55). Slr1916 is proposed to play a global regulatory role, and its

activity somehow limits the cellular level of PSI, the main sink for the Chl molecules in *Synechocystis* (56). We hypothesize that Slr1916 catabolizes unbound Chl accumulating in the membrane if Chl biosynthesis exceeds production of Chl-binding apoproteins (57). The activity of Slr1916 may therefore provide a feedback mechanism to synchronize the biosynthesis of Chl and Chl-binding proteins. As CycI and POR probably form an enzymatic complex (33), the greatly elevated level of POR in slr1916 mutants (Fig. 3D) might account for the increased activity of cyclase in the absence of Ycf54 and the higher stability of CycI^(SM) during nitrogen depletion. However, addressing the exact function of Slr1916 requires further study.

Conclusion

We have applied adaptive laboratory evolution to the Chl-deficient $\Delta ycf54$ mutant of *Synechocystis*, in combination with genomic sequencing, molecular genetics, phenotypic analyses, biochemical assays, and bioinformatic approaches. We have 1) shown that a point mutation allows the CycI cyclase to accumulate in the absence of Ycf54; 2) presented evidence that

Ycf54 regulates Chl biosynthesis by controlling the activity and level of CycI in response to fluctuating environmental factors; 3) demonstrated that the putative esterase Slr1916 has Chl dephosphorylase activity in vitro; and 4) investigated the evolution of O₂-dependent cyclase in *Prochlorococcus*, the most abundant photosynthetic organism on Earth.

Materials and Methods

Bacterial Strains and Growth Conditions. Bacterial strains described in this study are listed in SI Appendix, Table S1. *Synechocystis* strains were grown at 28 °C under constant illumination in BG11 medium buffered with 10 mM Tes, pH 8.2 (adjusted with KOH). Unless otherwise specified, light conditions were as follows: 10, 100, and 400 $\mu\text{mol photons}\cdot\text{m}^{-2}\cdot\text{s}^{-1}$, referred as LL, SL, and HL, respectively. Photoautotrophic liquid cultures were grown in air-bubbled 100-mL cylinders in a water-tempered growth chamber under SL. *Synechocystis* strains that are not photoautotrophic were grown in Erlenmeyer flasks on a rotary shaker in BG11 medium with 5 mM glucose under LL. For low-oxygen cultivation, cells were grown in Erlenmeyer flasks on a

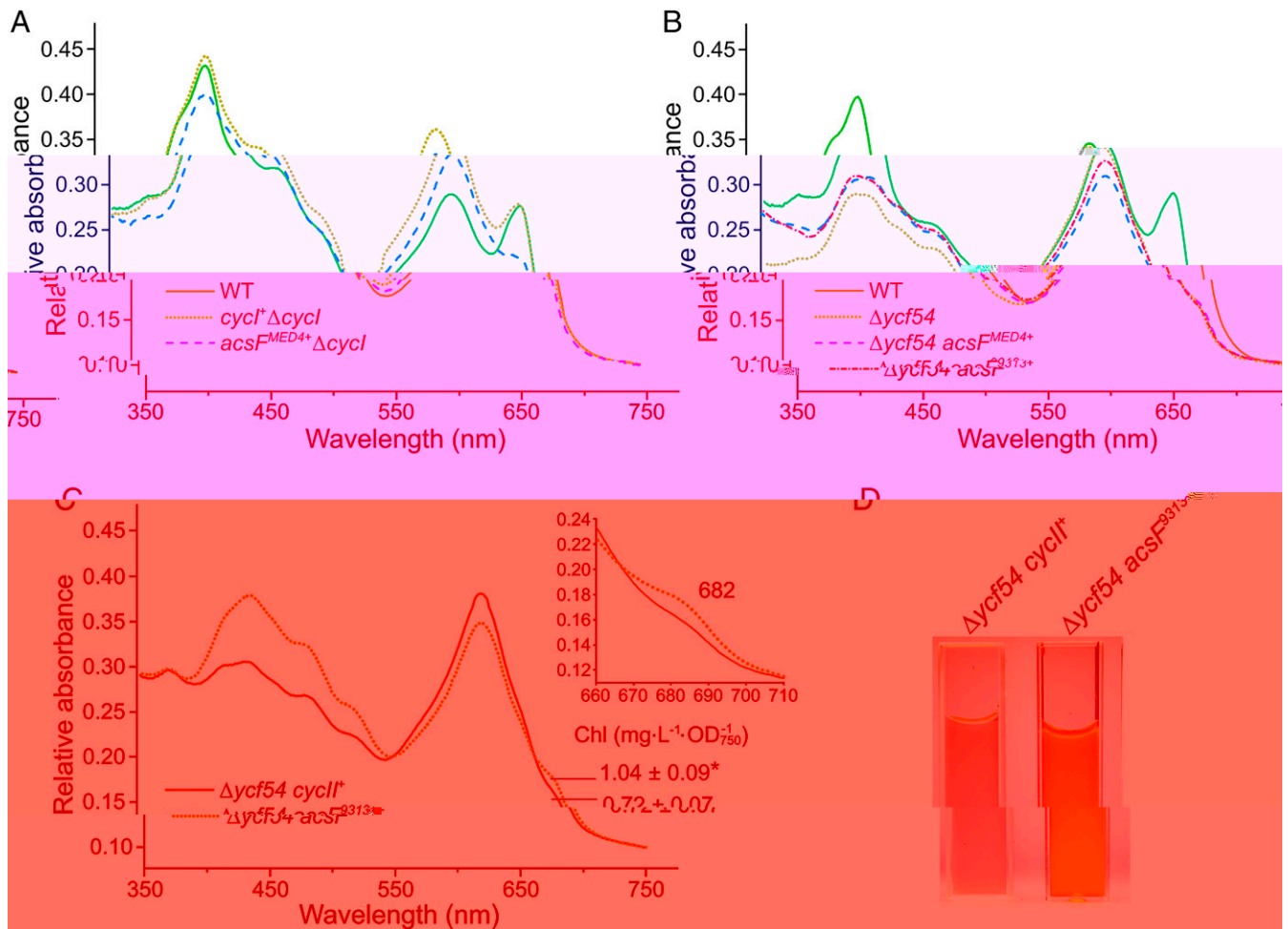


Fig. 10. Heterologous activity of *Prochlorococcus* cyclase enzymes in *Synechocystis*. Whole-cell absorption spectra of the described strains grown autotrophically under SL (A), mixotrophically under LL (B), and autotrophically under $30 \mu\text{mol photons}\cdot\text{m}^{-2}\cdot\text{s}^{-1}$ in a gas mixture of 2% O_2 and 0.5% CO_2 in N_2 (C). The Inset in C shows an expanded view of the absorption of Chl at 682 nm and Chl contents of the two strains (* $P < 0.02$, $n = 4$, Student's t test). (D) Visual comparison of pigmentation of the $\Delta\text{ycf}54 \text{ cycI}^+$ and $\Delta\text{ycf}54 \text{ acsF}^{9313}$ strains grown under the same conditions as in C.

under SL bubbled with sterile air and mixed using a magnetic stirrer. For plate-based drop growth assays, *Synechocystis* cell cultures were adjusted to $\text{OD}_{750\text{nm}}$ of 0.4 and diluted to 0.04 and 0.004. All three concentrations were spotted (5 μL) on solid medium, left to dry, and incubated under conditions as indicated in the text. *E. coli* strains were grown at 37°C in LB medium, and if required antibiotics were added at 30, 34, and $100 \mu\text{g}\cdot\text{mL}^{-1}$ for kanamycin, chloramphenicol, and ampicillin, respectively. *Rvi. gelatinosus* strains were grown at 30°C in PYS medium (58), and where required, kanamycin and rifampicin were added at 50 and $40 \mu\text{g}\cdot\text{mL}^{-1}$, respectively.

Construction of Plasmids and Bacterial Strains. Plasmids described in this study are listed in [SI Appendix, Table S1](#). Sequences of synthesized genes and primers described in this study are shown in [SI Appendix, Tables S3 and S4](#), respectively. The procedures for constructing plasmids and bacterial strains are described in [SI Appendix](#).

Genome Sequencing and Variant Calling. High-integrity *Synechocystis* genomic DNA was isolated, fragmented by nebulization with N_2 gas, and used for construction of a DNA library for paired-end sequencing using the Nextera DNA Library Preparation Kit (Illumina) with a median insert size of ~ 300 bp. The constructed library was subjected to 100-bp paired-end sequencing on an Illumina HiSeq 2000 platform according to the manufacturer's instructions. Variants were called using the mapping-based method, and those found in the suppressor mutants but not in the $\Delta\text{ycf}54$ strain were identified as putative suppressor mutations and listed in [SI Appendix, Table S2](#). Details of genomic DNA isolation, genome sequencing, and variant calling are described in [SI Appendix](#).

Protein Electrophoresis and Immunodetection. For native electrophoresis, solubilized membrane proteins were separated on 4 to 12% gels (59). Individual components of protein complexes were resolved by incubating the gel strip from the first dimension in 2% (wt/vol) SDS and 1% (wt/vol) dithiothreitol for 30 min at room temperature, and proteins were separated in the second dimension by SDS-PAGE in a denaturing 12 to 20% (wt/vol) polyacrylamide gel containing 7 M urea (60). The procedures for standard single-dimension SDS-PAGE, immunodetection, and assessment of antibody reactivity are detailed in [SI Appendix](#).

Whole-Cell Absorption Spectroscopy. *Synechocystis* whole-cell spectra were measured using a Shimadzu UV-3000 spectrophotometer and normalized to light scattering at 750 nm.

Pigment Extraction and Analysis by HPLC. Pigments were extracted from *Rvi. gelatinosus* cells with an excess of 0.2% (wt/vol) ammonia in methanol by vigorous shaking using a Mini-Beadbeater (BioSpec). Clarified pigment extracts were vacuum dried, reconstituted in 0.2% (wt/vol) ammonia in methanol, and analyzed by HPLC as previously described (61). *Synechocystis* Chl intermediates were analyzed by a previously described method (62).

Chl Dephnylase Assays. Anti-FLAG immunoprecipitation experiments were performed with the *Synechocystis* WT, FLAG-slr1916⁺, and slr1916-FLAG⁺ strains as described previously (9, 27). Recombinant Arabidopsis CLH1 protein was produced in *E. coli* BL21(DE3) as described previously (63), and clarified cell lysates were used as a positive control for the assay. *E. coli* MenH was overproduced with a His₆-tag in *E. coli* BL21(DE3) and purified by

Ni-affinity and size exclusion chromatography to determine whether it has nonspecific Chl dephytylase activity. Chl dephytylase assays were performed by adding 5 μ L of 500 μ M Chl a in acetone to 45 μ L of sample (FLAG-elution, CLH1 lysate, or purified MenH) so at a final concentration of 50 μ M pigment and 10% (vol/vol) acetone. The assay mixture was incubated at 35 $^{\circ}$ C for 30 min in darkness before stopping by adding 200 μ L of acetone, followed by vortexing and centrifugation. One hundred microliters of the resulting supernatant was diluted four times in methanol, and 100 μ L was loaded onto a Discovery HS C18 column (5 μ m; 250 \times 4.6 mm) and analyzed on an Agilent 1200 HPLC system as described previously (27).

Phylogenetic Analyses. A representative set of 1,048 publicly available cyanobacterial genome assemblies, quality-checked by the GTDB toolkit, version 1.0.2 (28, 64), was downloaded from the National Center for Biotechnology Information and utilized to create a custom BLAST database (65). Ycf54 from *Synechocystis* was used as a query for a tBLASTn search with a cutoff E value of 1e-10 against this database. All hits were automatically harvested and aligned using MAFFT, version 7 (66), to check their overall homology. The presence/absence of Ycf54 homologs was mapped to the current GTDB phylogenomic species tree of Cyanobacteria (based on 120 conserved proteins) to investigate their phylogenetic distribution among the LL- and HL-

adapted *Prochlorococcus* clades. To further compare the evolutionary scenarios between the AcsF protein and its parental organisms, we employed two phylogenetic analyses using an identical representative set of 103 organisms ranging from Acidobacteria, photosynthetic Proteobacteria, Chloroflexi, and Cyanobacteria to plant and algal plastids. The first tree was based on alignments of AcsF proteins, while the second tree was inferred from 13 universally conserved proteins selected from those used previously for studying plastid evolution (29). See details in [SI Appendix](#).

Data Availability. All study data are included in the article and/or [SI Appendix](#).

ACKNOWLEDGMENTS. G.E.C. and C.N.H. acknowledge support from Biotechnology and Biological Sciences Research Council Award BB/M000265/1 and State Key Laboratory of Microbial Metabolism Open Project Funding, Shanghai Jiao Tong University, China. A.H. acknowledges support from Royal Society University Research Fellowship Award URF/R1/191548. R.S., M.T., J.P., and B.Z. are supported by the Czech Science Foundation (Project 19-29225X). C.N.H. and R.S. are also supported by European Research Council Synergy Award 854126. We acknowledge the support of a Chinese Academy of Sciences Distinguished Visiting Scholar Fellowship.

- D. A. Bryant, C. N. Hunter, M. J. Warren, Biosynthesis of the modified tetrapyrroles—the pigments of life. *J. Biol. Chem.* **295**, 6888–6925 (2020).
- G. E. Chen et al., Complete enzyme set for chlorophyll biosynthesis in *Escherichia coli*. *Sci. Adv.* **4**, eaaq1407 (2018).
- R. J. Porra et al., Origin of the two carbonyl oxygens of bacteriochlorophyll a. Demonstration of two different pathways for the formation of ring E in *Rhodospira rubra* and *Rhodospira rubra* and a common hydratase mechanism for 3-acetyl group formation. *Eur. J. Biochem.* **239**, 85–92 (1996).
- V. Pinta, M. Picard, F. Reiss-Husson, C. Astier, Rubrivivax gelatinosus acsF (previously orf358) codes for a conserved, putative binuclear-iron-cluster-containing protein involved in aerobic oxidative cyclization of Mg-protoporphyrin IX monomethylester. *J. Bacteriol.* **184**, 746–753 (2002).
- E. N. Boldareva-Nuianzina, Z. Bláhová, R. Sobotka, M. Koblížek, Distribution and origin of oxygen-dependent and oxygen-independent forms of Mg-protoporphyrin monomethylester cyclase among phototrophic proteobacteria. *Appl. Environ. Microbiol.* **79**, 2596–2604 (2013).
- G. E. Chen, D. P. Canniffe, C. N. Hunter, Three classes of oxygen-dependent cyclase involved in chlorophyll and bacteriochlorophyll biosynthesis. *Proc. Natl. Acad. Sci. U.S.A.* **114**, 6280–6285 (2017).
- K. Minamizaki, T. Mizoguchi, T. Goto, H. Tamiaki, Y. Fujita, Identification of two homologous genes, chlA_I and chlA_{II}, that are differentially involved in isocyclic ring formation of chlorophyll a in the cyanobacterium *Synechocystis* sp. PCC 6803. *J. Biol. Chem.* **283**, 2684–2692 (2008).
- E. Peter et al., Differential requirement of two homologous proteins encoded by sll1214 and sll1874 for the reaction of Mg protoporphyrin monomethylester oxidative cyclase under aerobic and micro-oxic growth conditions. *Biochim. Biophys. Acta* **1787**, 1458–1467 (2009).
- S. Hollingshead et al., Conserved chloroplast open-reading frame ycf54 is required for activity of the magnesium protoporphyrin monomethylester oxidative cyclase in *Synechocystis* PCC 6803. *J. Biol. Chem.* **287**, 27823–27833 (2012).
- C. A. Albus et al., LCAA, a novel factor required for magnesium protoporphyrin monomethylester cyclase accumulation and feedback control of aminolevulinic acid biosynthesis in tobacco. *Plant Physiol.* **160**, 1923–1939 (2012).
- N. Yu et al., CS3, a Ycf54 domain-containing protein, affects chlorophyll biosynthesis in rice (*Oryza sativa* L.). *Plant Sci.* **283**, 11–22 (2019).
- S. Hollingshead et al., Synthesis of chlorophyll-binding proteins in a fully segregated *Δycf54* strain of the cyanobacterium *Synechocystis* PCC 6803. *Front. Plant Sci.* **7**, 292 (2016).
- D. Strenkert et al., Genetically programmed changes in photosynthetic cofactor metabolism in copper-deficient *Chlamydomonas*. *J. Biol. Chem.* **291**, 19118–19131 (2016).
- G. E. Chen, C. N. Hunter, Protochlorophyllide synthesis by recombinant cyclases from eukaryotic oxygenic phototrophs and the dependence on Ycf54. *Biochem. J.* **477**, 2313–2325 (2020).
- M. Castruita et al., Systems biology approach in *Chlamydomonas* reveals connections between copper nutrition and multiple metabolic steps. *Plant Cell* **23**, 1273–1292 (2011).
- M. Tichý et al., Strain of *Synechocystis* PCC 6803 with aberrant assembly of photosystem II contains tandem duplication of a large chromosomal region. *Front. Plant Sci.* **7**, 648 (2016).
- N. Tajima et al., Genomic structure of the cyanobacterium *Synechocystis* sp. PCC 6803 strain GT-S. *DNA Res.* **18**, 393–399 (2011).
- J. Kopečná et al., Porphyrin binding to Gun4 protein, facilitated by a flexible loop, controls metabolite flow through the chlorophyll biosynthetic pathway. *J. Biol. Chem.* **290**, 28477–28488 (2015).
- D. Vavilin, W. Vermaas, Continuous chlorophyll degradation accompanied by chlorophyllide and phytol reutilization for chlorophyll synthesis in *Synechocystis* sp. PCC 6803. *Biochim. Biophys. Acta* **1767**, 920–929 (2007).
- J. Kopečná et al., Lack of phosphatidylglycerol inhibits chlorophyll biosynthesis at multiple sites and limits chlorophyllide reutilization in *Synechocystis* sp. strain PCC 6803. *Plant Physiol.* **169**, 1307–1317 (2015).
- G. Allison, K. Gough, L. Rogers, A. Smith, A suicide vector for allelic recombination involving the gene for glutamate 1-semialdehyde aminotransferase in the cyanobacterium *Synechococcus* PCC 7942. *Mol. Gen. Genet.* **255**, 392–399 (1997).
- D. L. Ollis et al., The $\alpha\beta$ hydrolase fold. *Protein Eng. S.* **5**, 197–211 (1992).
- P. D. Carr, D. L. Ollis, $\alpha\beta$ hydrolase fold: An update. *Protein Pept. Lett.* **16**, 1137–1148 (2009).
- T. Tsuchiya et al., Chlorophyllase as a serine hydrolase: Identification of a putative catalytic triad. *Plant Cell Physiol.* **44**, 96–101 (2003).
- S. Schelbert et al., Pheophytin pheophorbide hydrolase (pheophytinase) is involved in chlorophyll breakdown during leaf senescence in *Arabidopsis*. *Plant Cell* **21**, 767–785 (2009).
- Y.-P. Lin, M.-C. Wu, Y. Y. Charn, Identification of a chlorophyll dephytylase involved in chlorophyll turnover in *Arabidopsis*. *Plant Cell* **28**, 2974–2990 (2016).
- J. W. Chidgey et al., A cyanobacterial chlorophyll synthase-HliD complex associates with the Ycf39 protein and the YidC/Alb3 insertase. *Plant Cell* **26**, 1267–1279 (2014).
- D. H. Parks et al., A standardized bacterial taxonomy based on genome phylogeny substantially revises the tree of life. *Nat. Biotechnol.* **36**, 996–1004 (2018).
- P. M. Shih et al., Improving the coverage of the cyanobacterial phylum using diversity-driven genome sequencing. *Proc. Natl. Acad. Sci. U.S.A.* **110**, 1053–1058 (2013).
- R. Aoki, T. Takeda, T. Omata, K. Ihara, Y. Fujita, MarR-type transcriptional regulator ChlR activates expression of tetrapyrrole biosynthesis genes in response to low-oxygen conditions in cyanobacteria. *J. Biol. Chem.* **287**, 13500–13507 (2012).
- S. Hollingshead, S. Bliss, P. J. Baker, C. Neil Hunter, Conserved residues in Ycf54 are required for protochlorophyllide formation in *Synechocystis* sp. PCC 6803. *Biochem. J.* **474**, 667–681 (2017).
- J. Herbst, A. Girke, M. R. Hajirezaei, G. Hanke, B. Grimm, Potential roles of YCF54 and ferredoxin-NADPH reductase for magnesium protoporphyrin monomethylester cyclase. *Plant J.* **94**, 485–496 (2018).
- D. Kauss, S. Bischof, S. Steiner, K. Apel, R. Meskauskiene, FLU, a negative feedback regulator of tetrapyrrole biosynthesis, is physically linked to the final steps of the Mg²⁺-branch of this pathway. *FEBS Lett.* **586**, 211–216 (2012).
- R. Sobotka, Making proteins green; biosynthesis of chlorophyll-binding proteins in cyanobacteria. *Photosynth. Res.* **119**, 223–232 (2014).
- D. Stuart et al., Aerobic barley Mg-protoporphyrin IX monomethyl ester cyclase is powered by electrons from ferredoxin. *Plants* **9**, 1157 (2020).
- D. Bollivar, I. Braumann, K. Berendt, S. P. Gough, M. Hansson, The Ycf54 protein is part of the membrane component of Mg-protoporphyrin IX monomethyl ester cyclase from barley (*Hordeum vulgare* L.). *FEBS J.* **281**, 2377–2386 (2014).
- N. Mochizuki, J. A. Brusslan, R. Larkin, A. Nagatani, J. Chory, *Arabidopsis* genomes uncoupled 5 (GUN5) mutant reveals the involvement of Mg-chelatase H subunit in plastid-to-nucleus signal transduction. *Proc. Natl. Acad. Sci. U.S.A.* **98**, 2053–2058 (2001).
- R. M. Larkin, J. M. Alonso, J. R. Ecker, J. Chory, GUN4, a regulator of chlorophyll synthesis and intracellular signaling. *Science* **299**, 902–906 (2003).
- R. Sobotka et al., Importance of the cyanobacterial Gun4 protein for chlorophyll metabolism and assembly of photosynthetic complexes. *J. Biol. Chem.* **283**, 25794–25802 (2008).
- P. A. Davison et al., Structural and biochemical characterization of Gun4 suggests a mechanism for its role in chlorophyll biosynthesis. *Biochemistry* **44**, 7603–7612 (2005).
- M. A. Verdecia et al., Structure of the Mg-chelatase cofactor GUN4 reveals a novel hand-shaped fold for porphyrin binding. *PLoS Biol.* **3**, e151 (2005).
- C. Formighieri, M. Ceol, G. Bonente, J. D. Rochaix, R. Bassi, Retrograde signaling and photoprotection in a gun4 mutant of *Chlamydomonas reinhardtii*. *Mol. Plant* **5**, 1242–1262 (2012).
- E. Peter, B. Grimm, GUN4 is required for posttranslational control of plant tetrapyrrole biosynthesis. *Mol. Plant* **2**, 1198–1210 (2009).

44. C. E. Bauer, A. Setterdahl, J. Wu, B. R. Robinson, "Regulation of gene expression in response to oxygen tension" in *The Purple Phototrophic Bacteria*, C. N. Hunter, F. Daldal, M. C. Thurnauer, J. T. Beatty, Eds. (Springer, 2009), pp. 707–725.
45. F. Partensky, L. Garczarek, *Prochlorococcus*: Advantages and limits of minimalism. *Annu. Rev. Mar. Sci.* **2**, 305–331 (2010).
46. Z. Sun, J. L. Blanchard, Strong genome-wide selection early in the evolution of *Prochlorococcus* resulted in a reduced genome through the loss of a large number of small effect genes. *PLoS One* **9**, e88837 (2014).
47. G. Roca et al., Genome divergence in two *Prochlorococcus* ecotypes reflects oceanic niche differentiation. *Nature* **424**, 1042–1047 (2003).
48. M. Jiang et al., Catalytic mechanism of SHCHC synthase in the menaquinone biosynthesis of *Escherichia coli*: Identification and mutational analysis of the active site residues. *Biochemistry* **48**, 6921–6931 (2009).
49. J. Gross et al., A plant locus essential for phyloquinone (vitamin K₁) biosynthesis originated from a fusion of four eubacterial genes. *J. Biol. Chem.* **281**, 17189–17196 (2006).
50. B. Orcheski, R. Parker, S. Brown, Pale green lethal disorder in apple (*Malus*) is caused by a mutation in the *PHYLLLO* gene which is essential for phyloquinone (vitamin K₁) biosynthesis. *Tree Genet. Genomes* **11**, 131 (2015).
51. T. W. Johnson et al., Recruitment of a foreign quinone into the A(1) site of photosystem I. I. Genetic and physiological characterization of phyloquinone biosynthetic pathway mutants in *Synechocystis* sp. pcc 6803. *J. Biol. Chem.* **275**, 8523–8530 (2000).
52. T. Wade Johnson et al., The *menD* and *menE* homologs code for 2-succinyl-6-hydroxyl-2,4-cyclohexadiene-1-carboxylate synthase and O-succinylbenzoic acid-CoA synthase in the phyloquinone biosynthetic pathway of *Synechocystis* sp. PCC 6803. *Biochim. Biophys. Acta* **1557**, 67–76 (2003).
53. J. R. Widhalm, C. van Oostende, F. Furt, G. J. C. Basset, A dedicated thioesterase of the Hotdog-fold family is required for the biosynthesis of the naphthoquinone ring of vitamin K₁. *Proc. Natl. Acad. Sci. U.S.A.* **106**, 5599–5603 (2009).
54. H. Ozaki, M. Ikeuchi, T. Ogawa, H. Fukuzawa, K. Sonoike, Large-scale analysis of chlorophyll fluorescence kinetics in *Synechocystis* sp. PCC 6803: Identification of the factors involved in the modulation of photosystem stoichiometry. *Plant Cell Physiol.* **48**, 451–458 (2007).
55. L. Yao et al., Pooled CRISPRi screening of the cyanobacterium *Synechocystis* sp. PCC 6803 for enhanced industrial phenotypes. *Nat. Commun.* **11**, 1666 (2020).
56. J. Kopečná, J. Komenda, L. Bučinská, R. Sobotka, Long-term acclimation of the cyanobacterium *Synechocystis* sp. PCC 6803 to high light is accompanied by an enhanced production of chlorophyll that is preferentially channeled to trimeric photosystem I. *Plant Physiol.* **160**, 2239–2250 (2012).
57. M. Pazdernik, J. Mareš, J. Pilný, R. Sobotka, The antenna-like domain of the cyanobacterial ferrochelatase can bind chlorophyll and carotenoids in an energy-dissipative configuration. *J. Biol. Chem.* **294**, 11131–11143 (2019).
58. K. V. Nagashima, K. Shimada, K. Matsuura, Shortcut of the photosynthetic electron transfer in a mutant lacking the reaction center-bound cytochrome subunit by gene disruption in a purple bacterium, *Rubrivivax gelatinosus*. *FEBS Lett.* **385**, 209–213 (1996).
59. I. Wittig, M. Karas, H. Schägger, High resolution clear native electrophoresis for isolation of membrane protein complexes. *Mol. Cell. Proteomics* **6**, 1215–1225 (2007).
60. M. Dobáková, R. Sobotka, M. Tichý, J. Komenda, Psb28 protein is involved in the biogenesis of the photosystem II inner antenna CP47 (PsbB) in the cyanobacterium *Synechocystis* sp. PCC 6803. *Plant Physiol.* **149**, 1076–1086 (2009).
61. G. E. Chen, D. P. Canniffe, E. C. Martin, C. N. Hunter, Absence of the *ccb3* terminal oxidase reveals an active oxygen-dependent cyclase involved in bacteriochlorophyll biosynthesis in *Rhodobacter sphaeroides*. *J. Bacteriol.* **198**, 2056–2063 (2016).
62. J. Pilný, J. Kopečná, J. Noda, R. Sobotka, Detection and quantification of heme and chlorophyll precursors using a high performance liquid chromatography (HPLC) system equipped with two fluorescence detectors. *Bio Protoc.* **5**, e1390 (2015).
63. T. Tsuchiya et al., Cloning of chlorophyllase, the key enzyme in chlorophyll degradation: Finding of a lipase motif and the induction by methyl jasmonate. *Proc. Natl. Acad. Sci. U.S.A.* **96**, 15362–15367 (1999).
64. P.-A. Chaumeil, A. J. Mussig, P. Hugenholtz, D. H. Parks, GTDB-Tk: A toolkit to classify genomes with the genome taxonomy database. *Bioinformatics* **36**, 1925–1927 (2019).
65. C. Camacho et al., BLAST+: Architecture and applications. *BMC Bioinformatics* **10**, 421 (2009).
66. K. Katoh, D. M. Standley, MAFFT multiple sequence alignment software version 7: Improvements in performance and usability. *Mol. Biol. Evol.* **30**, 772–780 (2013).